Cellular Imaging

DOI: 10.1002/anie.201210079

Using Fluorescent Post-Labeling To Probe the Subcellular Localization of DNA-Targeted Platinum Anticancer Agents**

*Song Ding, Xin Qiao, Jimmy Suryadi, Glen S. Marrs, Gregory L. Kucera, and Ulrich Bierbach**

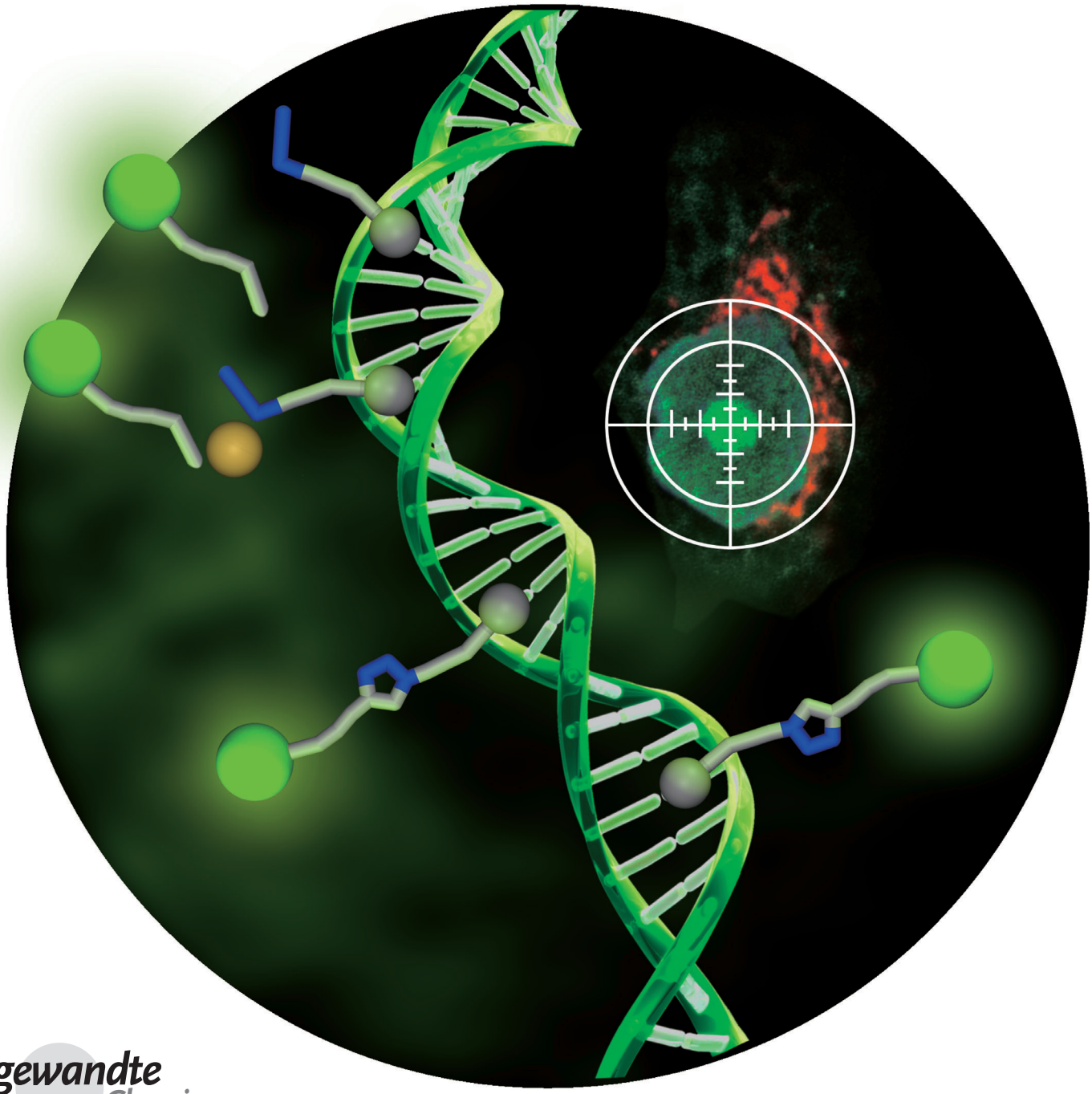

Adducts in the nuclear DNA are the major cause of cancer-cell death triggered by platinum-based anticancer drugs.[1] Thus, cellular uptake and accumulation, distribution, and trafficking between subcellular compartments and, ultimately, localization to the nucleus are crucial parameters in the mechanism of these agents. Several techniques have been used to monitor the intracellular distribution of platinum drugs. These include element-specific analytical methods and nondestructive absorption- or emission-based imaging techniques, as well as electron microscopy.[2,3] Fluorophore-tagged derivatives have provided insight into the uptake, distribution, and intracellular transformation of platinum drugs.[2] Such an approach has to take into consideration the organelle selectivity of the fluorophore, which may vary widely depending on parameters such as molecular weight, partition coefficient ($\log P$), amphiphilic character, and pK_a value.[4] Thus, one drawback of modifying platinum drugs with organic fluorophores is that such conjugates may, at least in part, mimic the properties of the reporter molecule.[5] This would be an undesired feature unless the fluorescent group itself is a functionally important part of the bioactive molecule. Likewise, bulky fluorophores may interfere with the DNA-binding mechanism of platinum drugs. To circumvent these problems, we have developed a method based on bioorthogonal ligation chemistry, which allowed us to fluorescently label platinum-acridine hybrid agents in lung cancer cells. Herein, we report the development of this technique and demonstrate, for the first time, that post-labeling is a powerful tool for detecting DNA-targeted platinum drugs in subcellular and subnuclear structures.

Platinum-acridines, represented by the prototypical compound **1** (Figure 1), are up to 500-times more cytotoxic to non-small-cell lung cancer cells than the drug cisplatin.[6] Studies in NCI-H460 cells suggest that the cytotoxicity produced by compound **1** is triggered by high levels of monofunctional-intercalative hybrid adducts in cellular DNA,[7] which is supported by recent results from chemogenomic screening in *S. cerevisiae*.[8] Unfortunately, direct fluorescent imaging of platinum-acridines in cancer cells is difficult because the

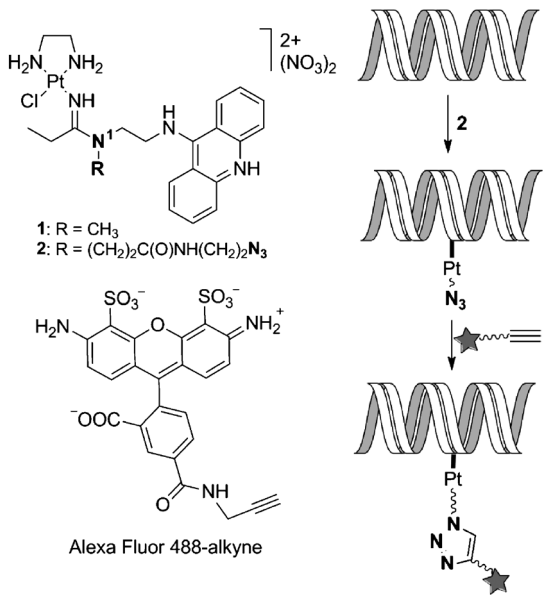

Figure 1. Formulas of compounds and reaction scheme for bioorthogonal fluorescent labeling of DNA-targeted platinum-acridine hybrid agents. Star = Alexa Fluor 488.

fluorescence of the 9-aminoacridine is severely quenched when intercalated into DNA (Supporting Information). [9] We therefore developed a method that allows for the labeling of platinum-acridines, in particular their DNA adducts, intracellularly using a high-performance fluorescent dye in conjunction with a copper-catalyzed azide–alkyne cycloaddition (CuAAC, click chemistry).[10,11] This strategy required modification of compound **1** with an alkyne or azide group in a way that would not interfere with the DNA-binding mode of the agent. Molecular models derived from the NMR solution structure of the hybrid adduct[12] (Supporting Information) suggest that the addition of a clickable group at the amidine N^1-methyl group in **1** (Figure 1), which is protruding out of the DNA major groove, should satisfy this requirement. While direct attachment of either functional group to this position using polymethylene linkers was incompatible with the metal and resulted in complex decomposition, our search identified a stable amide-linked azide derivative (compound **2**, Figure 1), which also showed excellent stability in aqueous media (see Supporting Information). Using gel-shift experiments to monitor DNA unwinding and CD spectropolarimetry, we confirmed that the azide-containing linker does not affect the geometry of the hybrid adduct (Supporting Information). Thus, compound **2** was chosen for our labeling technique in combination with the alkyne-modified form of the bright green-fluorescent dye Alexa Fluor 488 (Figure 1).

We established conditions for labeling the DNA adducts of compound **2** using a CuAAC reaction in a randomly platinated linearized plasmid. The procedure involved incubation of the DNA with compound **2** at varying platinum-to-nucleotide ratios (r_b) and reaction of the platinated DNA with Alexa Fluor 488-alkyne in the presence of a copper-based click-reaction buffer, followed by purification of the samples and analysis of the labeled DNA on agarose gels (for details see the Supporting Information). A fluorescent image of the

[*] S. Ding,[+] X. Qiao,[$] [+] Dr. J. Suryadi, Prof. U. Bierbach
Department of Chemistry, Wake Forest University
Winston-Salem, NC 27109 (USA)
E-mail: bierbau@wfu.edu
Dr. G. S. Marrs
Department of Biology, Wake Forest University
Winston-Salem, NC 27109 (USA)
Prof. G. L. Kucera
Department of Internal Medicine, Section on Hematology and Oncology, Wake Forest University Health Sciences
Winston-Salem, NC 27157 (USA)
[$] Permanent address: School of Pharmaceutical Sciences
Tianjin Medical University
Tianjin 300070 (PR China)
[+] These authors contributed equally to this work.
[**] This work was supported by the US National Institutes of Health (grant CA101880). X.Q. gratefully acknowledges support from the China Scholarship Council (grant no2011694010).
Supporting information for this article is available on the WWW under http://dx.doi.org/10.1002/anie.201210079.

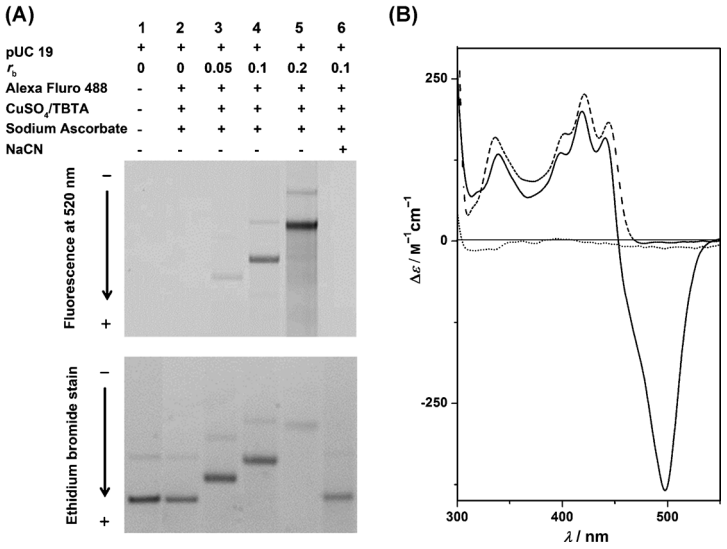

Figure 2. A) Electrophoretic analysis of copper-catalyzed ligation reactions between linearized (BamHI), platinated pUC19 plasmid DNA, and Alexa Fluor 488-alkyne with the reaction conditions indicated for each incubation (for details see Supporting Information). The top gel shows Alexa Fluor fluorescence monitored at 520 nm. Note the increase in band intensities and mobility shift with increasing platinum content. The band shift is caused by an accumulation of positive charge on the plasmid. The bottom gel is the same gel stained with ethidium bromide. Saturation of the DNA binding sites by Alexa Fluor-tagged platinum-acridine causes inefficient staining by ethidium bromide at $r_b = 0.2$. B) CD spectra recorded in the ICD region for unmodified DNA (••••), DNA modified with compound **2** (– – –), and DNA modified with compound **2** after ligation with Alexa Fluor 488-alkyne (——).

gel (at 520 nm) along with the ethidium bromide-stained gel is shown in Figure 2A. The bands on the gel show a pronounced increase in Alexa Fluor 488 fluorescence intensity with an increasing platinum-to-nucleotide ratio (lanes 3–5, top gel). To test whether the Alexa Fluor 488-alkyne was ligated to covalently bound platinum-acridine on the plasmid, a sample of fluorescently labeled DNA was incubated with NaCN, which reverses Pt-DNA adducts.[13] The complete disappearance of Alexa Fluor fluorescence in lane 6 (Figure 2A, top gel) and conversion of the platinated DNA into unmodified plasmid (Figure 2A, bottom gel, band of highest mobility) confirm that the platinum adducts were modified by the green-fluorescent dye.

CD spectra were recorded of native DNA globally modified with compound **2** before and after undergoing ligation with the Alexa Fluor dye (Figure 2B). The adducts formed by compound **2** give rise to positive Cotton effects in the 300–500 nm range, characteristic of the induced circular dichroism (ICD) of the intercalated acridine chromophore.[14] After labeling with Alexa Fluor 488-alkyne, the CD spectrum shows an additional negative ICD band at 498 nm, which mimics the absorbance spectrum of the dye, a consequence of the DNA chirality experienced by the ligated fluorophore. The hypsochromic shift of four nanometers observed for the acridine-based long-wavelength ICD bands in the labeled adduct relative to the unlabeled adduct of **2** suggests that ligation of the Alexa Fluor dye perturbs the hybrid binding mode, leading to partial unstacking of the acridine moiety.[12] By contrast, a comparison of the ICD signatures of DNA-bound compounds **1** and **2** shows that addition of the azide-containing side chain does not compromise acridine intercalation. This observation corroborates the notion that compound **2**, but not its fluorophore-tagged form, is a faithful mimic of compound **1**, which validates the post-labeling approach.

Next, we tested if the labeling strategy developed in cell-free DNA could be applied to whole cancer cells. For confocal fluorescence microscopy studies, NCI-H460 cells were incubated with **2** under conditions that were expected to produce high intracellular levels of platinum drug without killing the cells, as confirmed by the absence of the morphological hallmarks of apoptotic cell death.[15] Briefly, cultured cells were treated with three different doses (1, 5, or 25 μM) of compound **2** for three hours, washed, fixed in formalin, permeabilized, and incubated with CuAAC reaction buffer in the presence of Alexa Fluor 488-alkyne. Control experiments without platinum drugs were treated with fluorescent dye in the presence or absence of copper ions. Following exhaustive washing to remove the excess labeling mixture and co-staining with a nuclear dye (Hoechst 33342), cells were imaged by confocal fluorescence microscopy.

Images of platinum-treated NCI-H460 cells incubated with Alexa Fluor 488-alkyne and copper ions clearly demonstrate that this labeling method can be applied to whole cells (Figure 3A). Cells treated with compound **2** show a pronounced intensity increase in fluorescence emission relative to condition-matched controls, as a result of selective intracellular azide–alkyne ligation chemistry. Alexa Fluor 488 emission intensities in the nuclei of the treated cells ($n > 50$) show a clear correlation with increasing incubation concentrations of compound **2**, confirming that intracellular reaction with the azide-modified platinum/DNA adduct is the source of the fluorescence (see Supporting Information).

Platinum-azide-associated fluorescence was observed at high intensity within the nuclei and at a much lower intensity within the cytoplasm (for a detailed analysis of the distinct cellular regions, see the Supporting Information). Figure 3B shows co-localization images of Alexa Fluor 488 and the nuclear stain Hoechst 33342 within NCI-H460 cells during different stages of the cell cycle. During mitosis, the highest levels of green fluorescence were observed in the condensed, replicated chromatin, whereas cells in interphase show the strongest fluorescence signal across the entire nucleus. The highest fluorescence intensity in the nucleus during interphase was observed in the nucleoli, which are the sites of ribosomal RNA (rRNA) transcription during interphase.[16] An NCI-H460 cell imaged at high magnification shows the relative distribution of Alexa Fluor within the cell and confirms that compound **2** accumulates in the nucleus and nucleolus (Figure 4). Analysis of a large number of cells ($n =$ 40–50) shows that the emission in the 488 nm excitation channel has 50% higher relative intensity within the nucleolar regions compared to the surrounding chromatin (see Supporting Information).

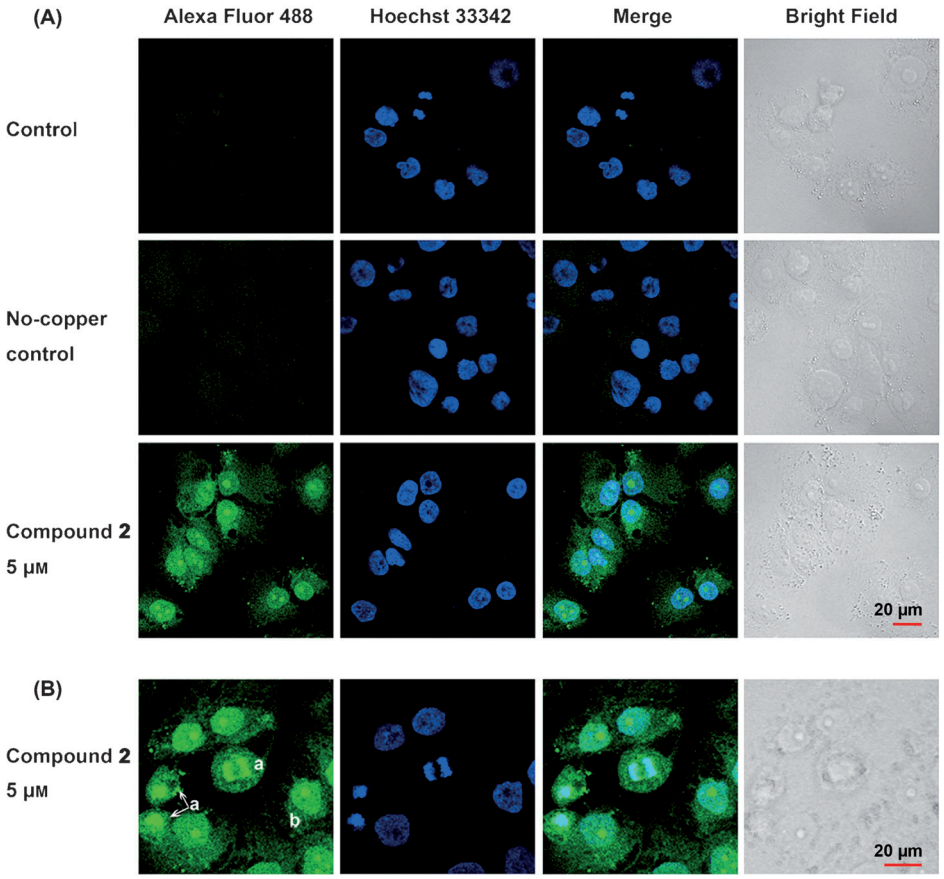

Figure 3. Imaging of compound **2** (5 μM) in fixed NCI-H460 lung cancer cells using Alexa Fluor 488-alkyne. Cells were co-stained with Hoechst 33342. A) Single confocal image planes of Alexa Fluor 488 (green), Hoechst 33342 (blue), the green and blue channels merged, and corresponding bright field image are shown for compound **2** treatment and control conditions. The control group was treated with Alexa Fluor 488-alkyne and copper-based ligation buffer. The no-copper control was treated with Alexa Fluor 488-alkyne in the absence of copper ions. B) Single confocal image plane of the cellular distribution of platinum-azide-associated fluorescence in NCI-H460 cells during mitosis (a) and interphase (b).

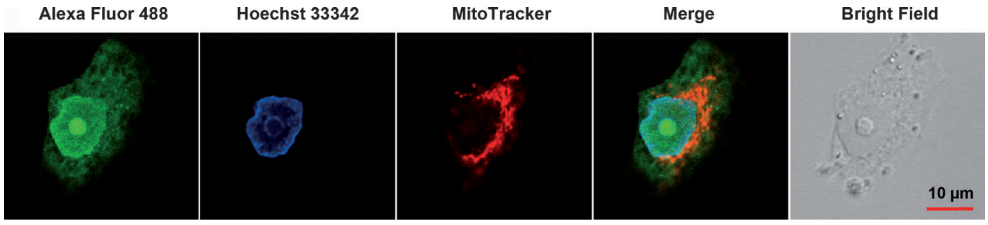

Figure 4. Intracellular distribution of compound **2** in an NCI-H460 cell in interphase. Cells were co-stained with nuclear (Hoechst 33342) and mitochondrial (MitoTracker Deep Red) dyes. The nucleolus, which is readily identified in the bright-field image as a nuclear region unstained by Hoechst dye, appears as an area of high fluorescence intensity in the Alexa Fluor 488 and the merged channel images.

In conclusion, the current study demonstrates that copper-mediated click chemistry is a powerful method for mapping the subcellular localization of a platinum-containing pharmacophore in fixed cancer cells. This was achieved by modifying a potent platinum-acridine anticancer agent so that a fluorophore could be ligated to it within cells. Compound **2** represents the first example of a platinum-based anticancer agent compatible with alkyne–azide ligation chemistry. The rapid accumulation of compound **2** in chromatin in the nucleus after only three hours of incubation is consistent with the high levels of platinum-DNA adducts seen previously in NCI-H460 cells by ICP-MS.[7] The imaging results support the notion that damage to nuclear DNA by platinum drugs is a major trigger of S-phase arrest and apoptosis in NCI-H460 cells.[8,17] The biological consequences of platinum-acridine localization to the nucleoli, on the other hand, remain elusive. Potential targets for platinum adduct formation in this dynamic, non-membrane-bound structure include transcriptionally active rRNA genes (rDNA) and nascent rRNA itself.[16] Nucleolar rRNA synthesis is an emerging target in anticancer drug development, and certain DNA intercalators have shown selective inhibition of rRNA transcription.[18,19] Notably, in deletion strains of *S. cerevisiae*, platinum-acridines elicit responses from genes involved in RNA metabolism, which suggests that inhibition of rRNA synthesis may contribute to the cell death produced by these agents.[8] Finally, we anticipate that this new imaging method could be extended to more biocompatible and ultrafast copper-free click chemistry, which could monitor platinum drug levels and localization in real-time within live cells.[20]

Received: December 18, 2012
Published online: February 20, 2013

Keywords: cancer · click chemistry · confocal microscopy · platinum drugs · post-labeling

[1] D. Wang, S. J. Lippard, *Nat. Rev. Drug Discovery* **2005**, *4*, 307–320.
[2] A. V. Klein, T. W. Hambley, *Chem. Rev.* **2009**, *109*, 4911–4920.
[3] L. E. Wedlock, S. J. Berners-Price, *Aust. J. Chem.* **2011**, *64*, 692–704.
[4] S. Trapp, R. W. Horobin, *Eur. Biophys. J.* **2005**, *34*, 959–966.
[5] X. J. Liang, D. W. Shen, K. G. Chen, S. M. Wincovitch, S. H. Garfield, M. M. Gottesman, *J. Cell. Physiol.* **2005**, *202*, 635–641.

[6] J. Suryadi, U. Bierbach, *Chem. Eur. J.* **2012**, *18*, 12926 – 12934.
[7] X. Qiao, A. E. Zeitany, M. W. Wright, A. S. Essader, K. E. Levine, G. L. Kucera, U. Bierbach, *Metallomics* **2012**, *4*, 645 – 652.
[8] K. Cheung-Ong, K. T. Song, Z. Ma, D. Shabtai, A. Y. Lee, D. Gallo, L. E. Heisler, G. W. Brown, U. Bierbach, G. Giaever, C. Nislow, *ACS Chem. Biol.* **2012**, *7*, 1892 – 1901.
[9] D. Fornasiero, T. Kurucsev, *Biophys. Chem.* **1985**, *23*, 31 – 37.
[10] Z. P. Demko, K. B. Sharpless, *Angew. Chem.* **2002**, *114*, 2214 – 2217; *Angew. Chem. Int. Ed.* **2002**, *41*, 2110 – 2113.
[11] S. B. Buck, J. Bradford, K. R. Gee, B. J. Agnew, S. T. Clarke, A. Salic, *Biotechniques* **2008**, *44*, 927 – 929.
[12] H. Baruah, M. W. Wright, U. Bierbach, *Biochemistry* **2005**, *44*, 6059 – 6070.
[13] S. A. Kane, S. J. Lippard, *Biochemistry* **1996**, *35*, 2180 – 2188.
[14] H. Kostrhunova, J. Malina, A. J. Pickard, J. Stepankova, M. Vojtiskova, J. Kasparkova, T. Muchova, M. L. Rohlfing, U. Bierbach, V. Brabec, *Mol. Pharm.* **2011**, *8*, 1941 – 1954.
[15] A. Saraste, K. Pulkki, *Cardiovasc. Res.* **2000**, *45*, 528 – 537.
[16] Y. W. Lam, L. Trinkle-Mulcahy, A. I. Lamond, *J. Cell Sci.* **2005**, *118*, 1335 – 1337.
[17] C. L. Smyre, G. Saluta, T. E. Kute, G. L. Kucera, U. Bierbach, *ACS Med. Chem. Lett.* **2011**, *2*, 870 – 874.
[18] D. Drygin, W. G. Rice, I. Grummt, *Annu. Rev. Pharmacol.* **2010**, *50*, 131 – 156.
[19] D. Drygin, A. Lin, J. Bliesath, C. B. Ho, S. E. O'Brien, C. Proffitt, M. Omori, M. Haddach, M. K. Schwaebe, A. Siddiqui-Jain, N. Streiner, J. E. Quin, E. Sanij, M. J. Bywater, R. D. Hannan, D. Ryckman, K. Anderes, W. G. Rice, *Cancer Res.* **2011**, *71*, 1418 – 1430.
[20] J. M. Baskin, J. A. Prescher, S. T. Laughlin, N. J. Agard, P. V. Chang, I. A. Miller, A. Lo, J. A. Codelli, C. R. Bertozzi, *Proc. Natl. Acad. Sci. USA* **2007**, *104*, 16793 – 16797.

